Inorg. Chem. **2005**, *44*, 5379–5387

Probing the Cytochrome P450-like Reactivity of High-Valent Oxo Iron Intermediates in the Gas Phase

M. Elisa Crestoni* and S. Fornarini

Dipartimento di Studi di Chimica e Tecnologia delle Sostanze Biologicamente Attive, Università di Roma "La Sapienza", P.le A. Moro 5, I-00185 Roma, Italy

Received October 8, 2004; Revised Manuscript Received May 2, 2005

Electrospray ionization in combination with Fourier transform ion cyclotron resonance spectrometry is used to prepare and characterize at a molecular level high-valent oxoiron intermediates formed in the reaction of [(TPFPP)Fe^{III}]Cl (TPFPP= *meso*-tetrakis(pentafluorophenyl)porphinato dianion) (**1**-Cl) with H_2O_2 in methanol. The intrinsic reactivity in the gas phase of the iron(IV) oxo porphyrin cation radical complex, [(TPFPP)$^{\bullet+}Fe^{IV}$=O]$^+$, has been probed toward selected substrates (S), chosen among naturally occurring and model compounds. Whereas CO and cyclohexane proved to be unreactive, olefins, sulfides, amines, and phosphites all undergo oxygen atom transfer in the gas phase yielding the reduction product **1** and/or an adduct ion ([**1**-S]$^+$). The reaction efficiencies show a qualitative correlation with the oxophilic character of the active site of S. A notable exception is nitric oxide, which displays a remarkably high reactivity, in line with the important role of NO reactions with iron porphyrin complexes. Furthermore, subsidiary information on the neat association reaction of **1** with selected ligands (L) has been obtained by a kinetic study showing that both the efficiency and the extent of ligation toward the naked ion **1** depend on the electron-donating ability of L.

Introduction

Several studies aimed at clarifying the mechanism of the catalytic cycles of monooxygenase enzymes have focused on the direct spectroscopic observation of the active species involved in the oxidative metabolism and on the development of biomimetic analogues unencumbered by the protein superstructure.[1−4]

High-valent oxoiron porphyrins have been invoked as the key intermediates responsible for the catalytic O−O bond activation by many heme enzymes, including cytochromes P450, NO synthase, and peroxidases.[5] The consensus intermediate of P450s, the oxoiron(IV) porphyrin π-cation radical **3**, referred to as compound I, effects a direct oxygen transfer process to a host of different substrates, such as alkanes, olefins, sulfides, and amines, ultimately reverting back to the reduced inactive resting form **1** (Scheme 1, where X^- is an anionic axial ligand). In the reaction cycle of peroxidases and catalases, compound I and an oxoiron (IV) porphyrin **4**,

Scheme 1

$$\underset{\textbf{1}\text{-X}}{Por\,Fe^{III}(X)} + Oxidant \rightarrow \underset{\textbf{2}\text{-X}}{Por\,Fe^{III}(X)\text{-}Oxidant} \rightarrow \underset{\textbf{3}\text{-X}}{Por^{\bullet+}Fe^{IV}(X)O} \rightarrow \underset{\textbf{4}\text{-X}}{Por\,Fe^{IV}(X)O}$$

* Author to whom correspondence should be addressed. E-mail: mariaelisa.crestoni@uniroma1.it.

(1) (a) Ortiz de Montellano, P. R. *Cytochrome P-450: Structure, Mechanism and Biochemistry*, 2nd ed.; Plenum Press: New York, 1995. (b) McLain, J.; Lee, J.; Groves, J. T. In *Biomimetic Oxidations Catalyzed by Transition Metal Complexes*; Meunier, B., Ed.; Imperial College Press: London, 2000; pp 91−170. (c) Montanari, F.; Casella, L. *Metalloporphyrins Catalyzed Oxidations*; Kluwer Academic Publishers: Dordrecht, The Netherlands, 1994. (d) Meunier, B.; Bernadou, J. *Struct. Bonding* **2000**, *97*, 1. (e) Watanabe, Y. In *The Porphyrin Handbook*; Kadish, K. M., Smith, K. M., Guilard, R., Eds.; Academic: New York, 2000; Vol. 4, Chapter 30, pp 97−117. (f) Groves, J. T. *Proc. Natl. Acad. Sci. U.S.A.* **2003**, *100*, 3569. (g) Sono, M.; Roach, M. P.; Coulter, E. D.; Dawson, J. H. *Chem. Rev.* **1996**, *96*, 2841.

(2) (a) Rohde, J.-U.; In, J.-H.; Lim, M. H.; Brennessel, W. W.; Bukowski, M. R.; Stubna, A.; Munck, E.; Nam, W.; Que, L., Jr. *Science* **2003**, *299*, 1037. (b) Nam, W.; Park, S.-E.; Lim, I. K.; Lim, M. H.; Hong, J.; Kim, J. *J. Am. Chem. Soc.* **2003**, *125*, 14674. (c) Grapperhaus, C. A.; Mienert, B.; Bill, E.; Weyhermüller, T.; Wieghardt, K. *Inorg. Chem.* **2000**, *39*, 5306.

(3) (a) Fujii, H. *Coord. Chem. Rev.* **2002**, *226*, 51. (b) Nakamoto, K. *Coord. Chem. Rev.* **2002**, *226*, 153.

(4) (a) Loew, G. H.; Harris, D. L. *Chem. Rev.* **2000**, *100*, 407. (b) Meunier, B.; de Visser, S. P.; Shaik, S. *Chem. Rev.* **2004**, *104*, 3947. (c) de Visser, S. P.; Shaik, S.; Sharma, P. K.; Kumar, D.; Thiel, W. *J. Am. Chem. Soc.* **2003**, *125*, 15779. (d) Guallar, V.; Friesner, R. *J. Am. Chem. Soc.* **2004**, *126*, 8501. (e) Green, M. T. *J. Am. Chem. Soc.* **1999**, *121*, 7939. (f) Rovira, C.; Kunc, K.; Hutter, J.; Ballone, P.; Parrinello, M. *J. Phys. Chem. A* **1997**, *101*, 8914.

(5) (a) Kellner, D. G.; Hung, S.-C.; Weiss, K. E.; Sligar, S. G. *J. Biol. Chem.* **2002**, *277*, 9641. (b) Schlichting, I.; Berendzen, J.; Chu, K.; Stock, A. M.; Maves, S. A.; Benson, D. A.; Sweet, R. M.; Ringe, D.; Petsko, G. A.; Sligar, S. G. *Science* **2000**, *287*, 1615. (c) Auclair, K.; Moënne-Loccoz, P.; Ortiz de Montellano, P. R. *J. Am. Chem. Soc.* **2001**, *123*, 4877.

10.1021/ic048595c CCC: $30.25
Published on Web 06/11/2005

called compound II, participate in the catalysis of organic compounds and hydrogen peroxide respectively via two sequential one-electron oxidations.[6]

Recently, other oxidants that are active prior to the formation of **3** have been invoked.[7] Oxidation of hydrocarbons has indeed been explained via the distinct existence of a catalyst−oxidant adduct **2** in native and mutant cytochromes P450, as well as in iron(III) porphyrin analogues (Scheme 1).[8]

Alternatively, a two-state reactivity model has been presented, whereby the mechanism and product distribution rely on a high-spin and a low-spin state of the active species **3**.[9]

As a result of their biological relevance and lability in nature, a variety of model complexes of compounds I and II have been prepared and characterized and also directly used in highly efficient and stereospecific industrial processes, as in the biocatalysis of chiral compounds.[2,8,10]

Groves et al. were the first to report a biomimetic epoxidation (promoted by a high-valent iron(IV) oxo porphyrin cation radical complex) using an iron(III) porphyrin complex **1** (e.g. [(TPP)Fe^{III}]Cl, TPP = *meso*-tetraphenylporphinato dianion) and iodosylbenzene (PhIO) as cooxidant.[11] Both the resistance toward oxidative degradation and the catalytic efficiency were then found to be considerably enhanced by functionalization with electron-withdrawing substituents at the *meso*- and/or the β-positions of the porphyrin ring which cause a large positive shift in the redox potential. In particular, (poly)halogenated iron porphyrin complexes are used as robust and powerful oxidants in a variety of oxygen atom transfer reactions.[12]

Also, numerous structure−reactivity investigations have recognized that the catalytic activity of metal complexes is dependent on several other factors, such as the identity of the terminal oxidant (e.g. hydroperoxides, peracids, iodosylbenzene, hypochlorites), the concentration of the substrate, the solvent (e.g. protic and aprotic solvent), pH, and the structure of the proximal ligand bound to the iron(III) porphyrin complexes.[13] Interestingly, it has been pointed out that the electron-donating ability of X (Scheme 1) significantly influences the nature, the lifetime, and the reactivity of iron porphyrin catalysts in epoxidation and hydroxylation reactions.[14]

In this context, gas-phase studies may have great potential in revealing the individual contributions of solvent, counterions, and aggregation/ligation, thus allowing the intrinsic reactivity of the active species to be elucidated at a molecular level. Most previous investigations on gaseous metal ion complexes were based on reactant species generated directly in the gas phase.[15] Herein, we prepared the oxoiron(IV) porphyrin cation radical intermediate **3**, [(TPFPP)$^{\bullet+}Fe^{IV}$=O]$^+$ (TPFPP = 5,10,15,20-tetrakis(pentafluorophenyl)porphinato dianion) ions in solution by the reaction of the iron(III) porphyrin chloride, [(TPFPP)Fe^{III}]Cl, and H_2O_2 in methanol at room temperature and then assayed its reactivity behavior in the gas phase, a dieletric medium resembling the local hydrophobic environment at the active site of cytochromes P450s. The use of H_2O_2 as the oxygen source in biomimetic oxidation processes is of particular interest because of its indiscriminate cellular toxicity besides its growing practical applications as an environmentally friendly reagent.[16]

Taking advantage of the ability of electrospray ionization (ESI) to gently transfer charged intermediates from solution to the gas phase, we decided to explore the oxygen atom transfer reactivity of isolated [(TPFPP)$^{\bullet+}Fe^{IV}$=O]$^+$ (**3**) as well as the ligand association ability of [(TPFPP)Fe^{III}]$^+$ (**1**) by using the ion manipulation and storage capabilities of Fourier transform ion cyclotron resonance mass spectrometry

(6) Dunford, H. B. *Heme Peroxidases*; Wiley: New York, 1999.

(7) (a) Vaz, A. D. N.; McGinnity, D. F.; Coon, M. J. *Proc. Natl. Acad. Sci. U.S.A.* **1998**, *95*, 3555. (b) Chandrasena, R. E. P.; Vatsis, K. P.; Coon, M. J.; Hollenberg, P. F.; Newcomb, M. *J. Am. Chem. Soc.* **2004**, *126*, 115.

(8) (a) Newcomb, M.; Shen, R.; Choi, S.-Y.; Toy, P. H.; Hollenberg, P. F.; Vaz, A. D. N.; Coon, M. J. *J. Am. Chem. Soc.* **2000**, *122*, 2677. (b) Nam, W.; Choi, S. K.; Lim, M. H.; Rohde, J.-U.; Kim, I.; Kim, J.; Kim, C.; Que, L., Jr. *Angew. Chem., Int. Ed.* **2003**, *42*, 109. (c) Suzuki, N.; Higuchi, T.; Nagano, T. *J. Am. Chem. Soc.* **2002**, *124*, 9622. (d) Nam, W.; Lim, M. H.; Lee, H. J.; Kim, C. *J. Am. Chem. Soc.* **2000**, *122*, 6641. (e) Collman, J. P.; Chien, A. S.; Eberspacher, T. A.; Brauman, J. I. *J. Am. Chem. Soc.* **2000**, *122*, 11098. (f) Wadhwani, P.; Mukherjee, M.; Bandyopadhyay, D. *J. Am. Chem. Soc.* **2001**, *123*, 12430. (g) Volz, T. J.; Rock, D. A.; Jones, J. P. *J. Am. Chem. Soc.* **2002**, *124*, 9724.

(9) (a) Schroeder, D.; Shaik, S.; Schwarz, H. *Acc. Chem. Res.* **2000**, *33*, 139. (b) Ogliaro, F.; de Visser, S. P.; Cohen, S.; Sharma, P. K.; Shaik, S. *J. Am. Chem. Soc.* **2002**, *124*, 2806. (c) Shaik, S.; de Visser, S. P.; Ogliaro, F.; Schwarz, H.; Schröder, D. *Curr. Opin. Chem. Biol.* **2002**, *6*, 556.

(10) (a) Groves, J. T.; Haushalter, R. C.; Nakamura, M.; Nemo, T. E.; Evans, B. J. *J. Am. Chem. Soc.* **1981**, *103*, 2884. (b) Penner-Hahn, J. E.; McMurry, T. J.; Renner, M. W.; Latos-Grazynski, L.; Eble, K. S.; Davis, I. M.; Balch, A. L.; Groves, J. T.; Dawson, J. H.; Hodgson, K. O. *J. Biol. Chem.* **1983**, *258*, 12761. (c) Traylor, T. G.; Kim, C.; Richards, J. L.; Xu, F.; Perrin, C. L. *J. Am. Chem. Soc.* **1995**, *117*, 3468.(d) Adam, W.; Heckel, F.; Saha-Moller, C. R.; Schreier, P. *J. Organomet. Chem.* **2002**, *661*, 17.

(11) Groves, J. T.; Nemo, T. E.; Myers, R. S. *J. Am. Chem. Soc.* **1979**, *101*, 1032.

(12) (a) Ostovic, D.; Bruice, T. C. *Acc. Chem. Res.* **1991**, *25*, 314. (b) Traylor, T. G.; Tsuchiya, S.; Byun, Y.-S.; Kim, C. *J. Am. Chem. Soc.* **1993**, *115*, 2775. (c) Dolphin, D.; Traylor, T. G.; Xie, L. Y. *Acc. Chem. Res.* **1997**, *30*, 251. (d) Fujii, H. *J. Am. Chem. Soc.* **1993**, *115*, 4641. (e) Goh, Y. M.; Nam, W. *Inorg. Chem.* **1999**, *38*, 914. (f) Chen, H. L.; Ellis, P. E., Jr.; Wijesekera, T.; Hagan, T. E.; Groh, S. E.; Lyons, J. E.; Ridge, D. P. *J. Am. Chem. Soc.* **1994**, *116*, 1086.

(13) (a) Urano, Y.; Higuchi, T.; Hirobe, M.; Nagano, T. *J. Am. Chem. Soc.* **1997**, *119*, 12008. (b) Nam, W.; Lim, M. H.; Oh, S.-Y. *Inorg. Chem.* **2000**, *39*, 5572. (c) Nam, W.; Jin, S. W.; Lim, M. H.; Ryu, J. Y.; Kim, C. *Inorg. Chem.* **2002**, *41*, 3647. (d) Nam, W.; Oh, S.-Y.; Sun, Y. J.; Kim, J.; Kim, W.-K.; Woo, S. K.; Shin, W. *J. Org. Chem.* **2003**, *68*, 7903.

(14) (a) Nam, W.; Lim, M. H.; Oh, S.-Y.; Lee, J. H.; Lee, H. J.; Woo, S. K.; Kim, C.; Shin, W. *Angew. Chem., Int. Ed.* **2000**, *39*, 3646. (b) Gross, Z.; Nimri, S.; Barzilay, C. M.; Simkhovich, I. *J. Biol. Inorg. Chem.* **1997**, *2*, 492.

(15) (a) Schroder, D.; Schwarz, H. *Angew. Chem., Int. Ed. Engl.* **1995**, *34*, 1973. (b) *Organometallic Ion Chemistry*; Freiser, B. S., Ed.; Kluwer Academic Publishers: Dordrecht, The Netherlands, 1996. (c) Blagojevic, V.; Jarvis, M. J. Y.; Flaim, E.; Koyanagi, G. K.; Lavrov, V. V.; Bohme, D. K. *Angew. Chem., Int. Ed.* **2003**, *42*, 4923. (d) Armentrout, P. B.; Tjelta, B. L. *Organometallics* **1997**, *16*, 5372. (e) Brönstrup, M.; Schröder, D.; Schwarz, H. *Chem.*—Eur. J. **1999**, *5*, 1176. (f) Chiavarino, B.; Crestoni, M. E.; Fornarini, S. *Chem.*—Eur. J. **2002**, *8*, 2740. (g) Perry, J. K.; Ohanessian, G.; Goddard, W. A. *Organometallics* **1994**, *13*, 1870. (h) Crestoni, M. E.; Fornarini, S. *Organometallics* **1996**, *15*, 5695.

(16) (a) Anastas, P. T.; Williamson, T. C. *Green Chemistry-Frontiers in Benign Chemical Syntheses and Processes*; Oxford University Press: Oxford, U.K., 1998. (b) Lane, B. S.; Burgess, K. *J. Am. Chem. Soc.* **2001**, *123*, 2933.

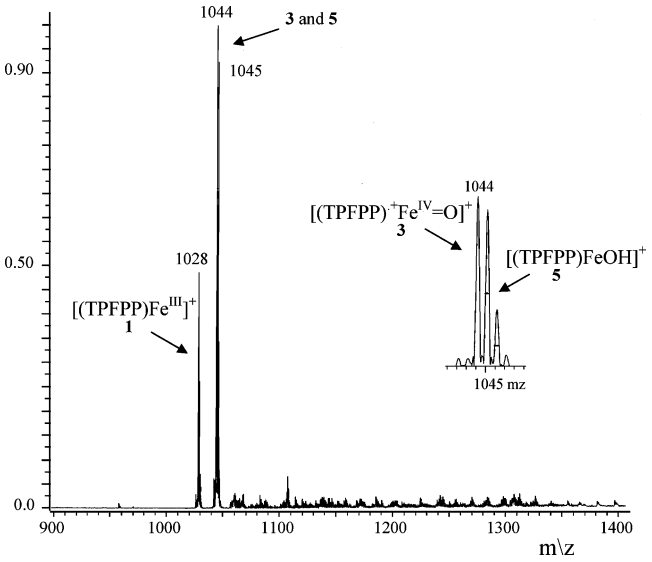

Figure 1. ESI(+) FT-ICR mass spectrum of a methanol solution of [(TPFPP)Fe^{III}]Cl (20 μM) and H_2O_2 (0.40 mM) at room temperature (300 K).

(FT-ICR-MS).[17,18] The selected neutrals were chosen among natural (NO) or model (olefins, sulfides, amines, phosphites) substrates of heme proteins and iron(III) porphyrin catalysts.

Experimental Section

Sample Preparation. Hydrogen peroxide (30% in water) and (5,10,15,20-Tetrakis(pentafluorophenyl)porphinato)iron(III) chloride, [(TPFPP)Fe^{III}]Cl (**1**-Cl), were obtained from Aldrich Chemical Co. *trans*-2-Butene, *cis*-2-butene, NO, and CO were high purity gases from Matheson Gas Products Inc. All other chemicals were research grade products obtained from commercial sources and used as received.

Stock solutions of **1**-Cl and the oxygen donor were typically prepared by dissolving **1**-Cl to make a 1 mM solution in methanol and by diluting hydrogen peroxide to make a 0.1 mM solution in bidistilled water. The reaction solution to be submitted to ESI (A) was prepared by slowly adding H_2O_2 to a methanol solution of **1**-Cl (20 μM) at room temperature up to a nominal 0.40 mM concentration of H_2O_2. These experimental conditions resulted in a good compromise between a fast and efficient formation of high-valent iron intermediates and an acceptable stability of the solutions. The resulting mixture (A) was submitted to ESI, and mass analysis showed two prominent species assigned to **3**, [(TPFPP)$^{\bullet+}$Fe^{IV}=O]$^{+}$ (m/z = 1044), and **5**, [(TPFPP)Fe(OH)]$^{+}$ (m/z = 1045), as shown in Figure 1. The **3**/**5** intensity ratio of the two ions was found to decrease from ca. 2, from freshly prepared A, to less than 0.2 from aged solutions. At 70 min after mixing, **5** was still abundant, whereas **1** and **3** were almost totally converted to a new iron-containing species (m/z = 1106). Fresh solutions kept in an ice bath were found to be stable for hours.

Reactions carried out with larger H_2O_2/**1**-Cl molar ratio (50−100 instead of 20) resulted in rather unstable products and gave rise to a peak assigned to (porphyrin)Fe^{III} *N*-oxide^{+} ions, [(TPFPP-*N*-O)Fe^{III}]$^{+}$ (m/z = 1044), rather than **3**.

When H_2O_2 and **1**-Cl were mixed in the presence of a selected substrate S (1.0 μM) (S = Me_2S, PhI, PhSMe, PPh_3) in the same solution, high yields of the corresponding oxoiron porphyrin adducts [(TPFPP)Fe(S)O]$_{sol}^{+}$ were afforded, except in the case of iodobenzene, which caused complete reduction of **3** to **1**. The degree of collision-induced dissociation (CID) during the transfer of [(TPFPP)Fe(S)O]$_{sol}^{+}$ to the gas phase was minimized by careful tuning of the cone voltage/capillary to skimmer potential difference.

Alternatively, [(TPFPP)Fe(S)O]$_{gas}^{+}$ adduct ions were obtained by the association reaction between electrosprayed **3** and volatile compounds (S = *c*-C_6H_{10}, Me_2NH, Me_2S) in the FT-ICR cell. The adduct ions formed in either way, [(TPFPP)Fe(S)O]$_{sol}^{+}$ or [(TPFPP)-Fe(S)O]$_{gas}^{+}$, were sampled by ligand transfer reactions with a series of compounds N (N = Me_2NH, pyridine) leaked at the stationary pressure of 1×10^{-8}−1×10^{-7} mbar.

Instrumental Details. All experiments were run with a Bruker BioApex 4.7T FT-ICR mass spectrometer equipped with an Analytica of Branford Inc. electrospray ionization source, a cylindrical infinity cell, and two pulsed valves. Analyte solutions were infused into a 50 μm i.d. fused-silica capillary at a rate of 200 μL h^{-1} by a syringe pump, and ions were accumulated in a rf-only hexapole ion guide for 0.6 s. The ion population was pulsed into the ICR cell at room temperature, and the reactant ion of interest was isolated by broad-band radio frequency pulses and exposed to a neutral reagent leaked by a needle valve at constant pressure (1×10^{-8}−2×10^{-7} mbar). Pressure readings were obtained from a Bayard-Alpert ionization gauge, calibrated by using the rate constant $k = 1.1 \times 10^{-9}$ cm^3 s^{-1} for the reference reaction $CH_4^{\bullet+} + CH_4 \rightarrow CH_5^{+} + CH_3^{\bullet}$ and corrected for different response factors.[19,20] Corrections for (^{13}C) isotopic contributions were effected whenever the ion of interest appeared as an isotopic cluster contaminated by the presence of adjacent or overlapping peaks from another ionic species. In this case of closely frequency spaced peaks, the use of ion separation techniques was avoided to prevent any unplanned excitation of the selected ion.

Pseudo-first-order-rate constants were obtained from the slope of the semilog decrease of the reactant ion signal vs time and divided by the known pressure of the neutral to derive bimolecular rate constants (k_{exp}). The rate constants shown in Tables 1−3, obtained as average values from at least three determinations at different neutral pressures, were also expressed as percentages (ϕ = efficiency) of the collision rate constant (k_{coll}) calculated by the parametrized trajectory theory.[21] The reproducibility of k_{exp} values was good, while the estimated error (±30%) is mainly related to the uncertainty of neutral concentrations.

Branching ratios for parallel reaction pathways were obtained from the extrapolation of product ion intensities at initial times, to avoid interference from consecutive processes.

The rate constants of sequential reactions were evaluated by a kinetic fitting program.[22]

Results and Discussion

Synthesis and Characterization. The addition of H_2O_2 to a methanol solution of [(TPFPP)Fe^{III}]Cl (**1**-Cl) at room temperature yielded a solution sampled by ESI-FT-ICR soon

(17) (a) Fenn, J. B.; Mann, M.; Meng, C. K.; Wong, S. F.; Whitehouse, C. M. *Science* **1989**, *246*, 64. (b) *Electrospray Ionization Mass Spectrometry, Fundamentals, Instrumentation and Applications*; Cole, R. B., Ed.; Wiley-Interscience: New York, 1997. (c) Klassen, J. S.; Ho, Y.; Blades, A. T.; Kebarle, P. *Adv. Gas-Phase Ion Chem.* **1998**, *3*, 255. (d) Traeger, J. C. *Int. J. Mass Spectrom.* **2000**, *200*, 387.
(18) Marshall, A. G.; Hendrickson, C. L.; Jackson, G. S. *Mass Spectrom. Rev.* **1998**, *17*, 1.
(19) Meot-Ner, M. In *Gas-Phase Ion Chemistry*; Bowers, M. T., Ed.; Academic Press: New York, 1979; Vol. 1.
(20) Bartmess, J. E.; Georgiadis, R. M. *Vacuum* **1983**, *33*, 149.
(21) Su, T.; Chesnavich, W. J. *J. Chem. Phys.* **1982**, *76*, 5183.
(22) Nicoll, J. B.; Dearden, D. V. *KinFit*, v.1.0; Department of Chemistry and Biochemistry, Brigham Young University: Provo, UT, 1997.

after preparation. ESI-MS is a powerful tool for mechanistic studies in homogeneous catalysis by means of its ability to bring complicated or even loosely bound organometallic intermediates from solution to the gas phase.[23] Besides the direct observation of catalytically competent species, FT-ICR-MS allows one to detect relatively short-lived intermediates and to assay their reactivity with selected molecules.

A representative spectrum of the electrosprayed reaction solution is shown in Figure 1. In addition to the precursor iron(III) porphyrin ion **1** ($m/z = 1028$), two prominent ionic species, both displaying the characteristic isotopic pattern of an iron porphyrin species similar to **1**, could be detected. The first one, centered at $m/z = 1044$, can be assigned to **3** and a second one, centered at $m/z = 1045$, assigned to **5**. According to the proposed heterolytic O−O bond cleavage of hydroperoxides by iron porphyrins in protic solvents, a high-valent iron(IV) oxo porphyrin cation radical $[(TPFPP^{\bullet+}\text{-}Fe^{IV}{=}O]^+$ (**3**) is likely to be present in solution (eq 1a).[10c] If no oxidable substrates are added to the solution, as in the present case, **3** may turn into to a hydroxoiron species $[TPFPPFe^{IV}{-}OH]^+$ (**5**) through hydroperoxide oxidation (eq 1b). However, the use of the electron-deficient iron porphyrin complex **1**, already found to remarkably decrease the rate of this side reaction with respect to iron porphyrin complexes lacking this feature, afforded only a moderate yield of **5** and also prevented the relative amounts of these cationic intermediates to drastically change with time.

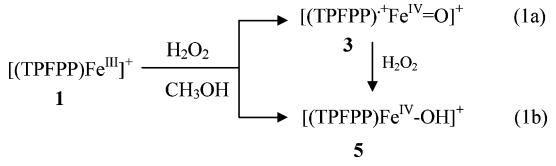

Altogether, the ionic species **3** and **5** display the isotopic cluster shown in the insert of Figure 1. Systematic subtraction of the isotopic contribution(s) of **3** from the intensity of **5** allowed us to determine the relative amount of the two species in each spectrum. To avoid unplanned excitation, both ions **3** and **5** were mass selected together for accurate mass analysis and for probing their features in the gas phase. The reactions of $[(TPFPP)Fe^{III}]^+$ (**1**) and of (porphyrin)Fe^{III} *N*-oxide$^+$ ions, $[(TPFPP{-}N{-}O)Fe^{III}]^+$, toward selected gaseous compounds have also been investigated. The gas-phase ion chemistry of all sampled intermediates matched with their proposed structures as illustrated in the following sections.

Oxygen Atom Transfer in the Gas Phase. Reactivity of $[(TPFPP)^{\bullet+}Fe^{IV}{=}O]^+$ toward Inorganic and Organic Substrates. Several mass spectrometric studies have investigated the structure, stability, and reactivity of small metal ion complexes in the gas phase.[15,24] The reactivity of metal oxide cations MO^+ (M = Mn, Fe, Co, Ni) generated in the gas phase revealed the ability of these species to oxidize a variety of simple molecules, including dihydrogen and methane.[15a] Attempts to add an oxo ligand to iron porphyrin ions in the gas phase have been successful in the reaction of NO_2 with the molecular anions of iron porphyrins, whereas the corresponding cationic oxo species could not be directly detected but only inferred as transient species along a reaction pathway.[25]

Table 1. Gas-Phase Reactivity of Selected Substrates (S) with $[(TPFPP)^{\bullet+}Fe^{IV}{=}O]^+$ (**3**) Generated by $[(TPFPP)Fe^{III}]Cl$ and H_2O_2 in CH_3OH, at Room Temperature

S (IP)[a]	$k_{exp(1)}$[b,c]	$\phi_{(1)}$[d]	$k_{exp(2)}$[b,e]	$\phi_{(2)}$[d]	product ions $[(TPFPP)Fe^{III}]^+$/ $[(TPFPP)Fe(S)O]^+$
NO (9.26)	0.18	2.5			80/20
NO_2 (9.59)	0.12	2.0			100/0
c-C_6H_{10} (8.95)	0.19	2.0			75/25
(*Z*)-2-butene (9.11)	0.10	0.94			90/10
(*E*)-2-butene (9.10)	0.08	0.74			90/10
Me_2S (8.69)	0.45	3.5			30/70
Me_2NH (8.24)	0.80	7.0	0.12	1.0	0/100
C_5H_5N (9.26)	0.83	6.1	0.19	1.4	0/100
$P(OMe)_3$ (8.4)	5.5	49			90/10

[a] Ionization potentials (IP) in eV are given in parentheses. [b] Phenomenological rate constants in units of 10^{-10} cm^3 molecule^{-1} s^{-1}, at the temperature of the FT-ICR cell of 300 K. The estimated error is ±30%. The internal consistency of the data is within ±10%. [c] The following reactants failed to react with **3**: CO; cyclohexane; N_2O; benzene. [d] $\phi = k_{exp}/k_{coll} \times 100$. Collision rate constants (k_{coll}) evaluated with the parametrized trajectory theory.[21] [e] Reaction step: $[(TPFPP)Fe(S)O]^+ + S \rightarrow [(TPFPP)Fe(S)O(S)]^+$.

In solution, several examples of oxygenations at a heteroatom using model iron porphyrins and cytochrome P450 are known, including sulfur, nitrogen, and trivalent phosphorus oxidations, where the conversion of a substrate containing a heteroatom to its corresponding heteroatom oxide is reported to occur.[26] Under experimental conditions similar to the ones adopted in this study, the $[(TPFPP)Fe^{III}]$-Cl catalysis of H_2O_2-induced oxidation in solution of olefins to epoxides and of sulfides to sulfoxides/sulfones has been suggested to involve **3** as the active species.[10c,14a,27]

In this study, when **3** generated in solution is carried into the gas phase, free from solvent molecules, conveyed into the FT-ICR cell, and assayed by its reactivity with neutral S, two different reaction channels are observed, whose relative extent depends on the nature of the substrate S (Table 1 and eq 2), namely, (1) reduction to **1** concomitant with oxygen atom transfer to S (eq 2a) and (2) direct association of S to form an adduct ion, $[(TPFPP)Fe(S)O]^+$ (eq 2b), possibly stabilized by collisional and/or radiative cooling.[28] It should be noted that the adduct ion, $[(TPFPP)Fe(S)O]^+$, is primarily characterized by its m/z ratio; therefore, the

(23) (a) Colton, R.; D'Agostino, A.; Traeger, J. C. *Mass Spectrom. Rev.* **1995**, *14*, 79. (b) Hilderling, C.; Adlhart, C.; Chen, P. *Angew. Chem., Int. Ed.* **1998**, *37*, 2685. (c) Sabino, A. A.; Machado, A. H. L.; Correia, C. R. D.; Eberlin, M. N. *Angew. Chem., Int. Ed.* **2004**, *43*, 2514. (d) Chen, P. *Angew. Chem., Int. Ed.* **2003**, *42*, 2832. (e) Bossio, R. E.; Hoffman, N. W.; Cundari, T. R.; Marshall, A. *Organometallics* **2004**, *23*, 144. (f) Feichtinger, D.; Plattner, D. A. *Chem.*—Eur. J. **2001**, *7*, 591. (g) Gerdes, G.; Chen, P. *Organometallics* **2004**, *23*, 3031.

(24) Armentrout, P. B. *Acc. Chem. Res.* **1995**, *28*, 430.

(25) (a) Irikura, K. K.; Beauchamp, J. L. *J. Am. Chem. Soc.* **1991**, *113*, 2767. (b) Chen, H. L.; Hagan, T. E.; Groh, S. E.; Ridge, D. P. *J. Am. Chem. Soc.* **1991**, *113*, 9669.

(26) (a) Goto, Y.; Watanabe, Y.; Fukuzumi, S.; Jones, J. P.; Dinnocenzo, J. P. *J. Am. Chem. Soc.* **1998**, *120*, 10762. (b) Baciocchi, E.; Gerini, M. F.; Lapi, A. *J. Org. Chem.* **2004**, *69*, 3586. (c) Lei, J.; Trofimova, N. S.; Ikeda, O. *Chemistry Lett.* **2003**, *32*, 610.

(27) Nam, W.; Lim, M. H.; Lee, H. J.; Kim, C. *J. Am. Chem. Soc.* **2000**, *122*, 6641.

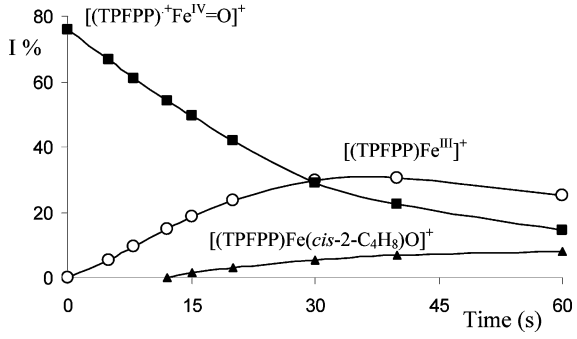

Figure 2. Time dependence of relative ion intensities for $[(TPFPP)^{\bullet+}Fe^{IV}{=}O]^+$ ions at $m/z = 1044$ (■), $[(TPFPP)Fe^{III}]^+$ ions at $m/z = 1028$ (○), and $[(TPFPP)Fe(cis\text{-}2\text{-}C_4H_8)O]^+$ ions at $m/z = 1100$ (▲). The *cis*-2-C_4H_8 pressure was 1.0×10^{-7} mbar.

bonding features of S, either part of a single ligand SO or present as a separate trans-axial ligand, are not yet established.

$$[(TPFPP)^{\bullet+}Fe^{IV}{=}O]^+ \quad (\mathbf{3}) \quad + \; S \;\rightarrow\; \mathbf{1} + S\text{-}O \qquad (2a)$$

$$\rightarrow\; [(TPFPP)Fe(S)O]^+ \quad (\mathbf{6}) \qquad (2b)$$

The ion abundance of **3** has been found to decay exponentially with time until complete conversion into products, as shown by the ion intensity profiles as a function of time for the *cis*-2-butene reaction (Figure 2). The second-order rate constants, $k_{exp(1)}$, and the reaction efficiencies ($\phi_{(1)}$), defined as the ratio of $k_{exp(1)}$ to the collision frequency k_c,[21] as well as the branching ratio of the primary product ions of eq 2 are summarized in Table 1. These values were found to be invariant with respect to the partial pressure of S and of an added inert gas (Ar).[29] O-atom transfer (eq 2a) takes place from electrosprayed **3** to tested gaseous compounds, including olefins, nitrogen oxides, sulfur, and phosphorus compounds, with the exception of amines, which react exclusively by the addition pathway (eq 2b). The latter route may be followed by a consecutive association reaction to give the bis-ligated adduct $[(TPFPP)Fe(S)O(S)]^+$ (S = dimethylamine, pyridine), whose rate constant ($k_{exp(2)}$) and efficiency ($\phi_{(2)}$) is also shown in Table 1. The notation used to represent the product ion, $[(TPFPP)Fe(S)O(S)]^+$, which is primarily characterized by its *m*/*z* ratio, is meant to simply indicate the addition of two S molecules, their coordination features yet unknown. Likewise, the reduction product of reaction 2a, **1**, may react further with S leading to adduct ions, $[(TPFPP)Fe^{III}S]^+$. This addition process, which mimics the binding of substrate molecules to the axial sites of the resting form of the heme enzymes, will be discussed in a following section.

Several small molecules ($S = O_2$, CO, N_2O, cyclohexane, and benzene) do not show any tendency to react according to routes 2a and 2b nor toward any C−H and C−C activation processes, at an appreciable rate under ICR conditions ($k_{exp} < 10^{-12}$ cm^3 molecule^{-1} s^{-1}). This is obviously a result of the presence of the porphyrin ligand, namely a clear manifestation of ligand effects, routinely used to control the reactivity of metal complexes. The porphyrin ligand exerts such an effect on the gaseous iron complex as to inhibit any reactivity by the substrates that are less susceptible to undergo oxidation. These same substrates, e.g. cyclohexane and benzene, are in fact easily oxidized by bare FeO^+ in the gas phase.[30] In this view, it is remarkable that the heme cofactor performs the catalytic oxidations within the highly specialized environment of the P450 enzyme. Moreover, the evidence that **3** does not show any appreciable bias to unimolecular dissociation proves its noticeable stability, even when trapped for 100−500 s in the presence of an unreactive gas, e.g. CO at 2×10^{-7} mbar. Control experiments employing the isobaric (porphyrin)Fe^{III}*N*-oxide$^+$ ions, $[(TPFPP{-}N{-}O)Fe^{III}]^+$, demonstrate that this isomeric species is unable to oxidize any of the selected substrates of Table 1. This reactivity behavior is expected because of the lack of an $Fe^{IV}O$ moiety in $[(TPFPP{-}N{-}O)Fe^{III}]^+$, which rather shows comparable reactivity as ion **1**, yielding only addition products, $[(TPFPP{-}N{-}O)Fe^{III}(S)]^+$.

Similarly, the hydroxoiron species **5** resulted totally unreactive toward all compounds listed in Table 1, and thus, its constant abundance was omitted for the sake of clarity in all kinetic plots. Indeed, this finding could be expected given the substantially decreased reactivity of gaseous $FeOH^+$ toward element hydrides with respect to FeO^+.[15e]

When **3** is allowed to react with nitric oxide, oxygen atom transfer is the dominant channel (90%), which implies the oxidation of nitrogen monoxide to nitrogen dioxide (eq 3a). The latter compound is thermochemically favored by a $\Delta_f H°$ difference of approximately 57 kJ mol^{-1}.[31] The ensuing product ion, **1**, undergoes addition of NO ultimately leading to $[(TPFPP)Fe^{III}NO]^+$ (eq 3b).

$$\mathbf{3} + NO \rightarrow \mathbf{1} + NO_2 \qquad (3a)$$

$$\mathbf{1} + NO \rightarrow [(TPFPP)Fe^{III}NO]^+ \qquad (3b)$$

In our view, the reactivity with NO deserves interest because of the physiological significance of nitric oxide, which is related to its interaction with the heme cofactor.[32] For example, reduction of high-valent intermediates of heme enzymes, modeled by the present $[(TPFPP)^{\bullet+}Fe^{IV}{=}O]^+$ ion, by nitric oxide has recently been suggested as a protective process against inflammation.[32b]

As already mentioned, the reverse process of reaction 3a was suggested to occur under ICR conditions by Ridge et al., who proposed a two-step mechanism involving the intermediacy of an elusive oxo species in the formation

(28) (a) Dunbar, R. C. *Mass Spectrom. Rev.* **2004**, *23*, 127. (b) Dunbar, R. C.; McMahon, T. B. *Science* **1998**, *279*, 194.
(29) Bruce, J. E.; Eyler, J. R. *J. Am. Soc. Mass. Spectrom.* **1992**, *3*, 733.
(30) Stöckigt, D.; Schwarz, H. *Chem. Ber.* **1994**, *127*, 2499.
(31) Hunter, E. P.; Lias, S. G. *NIST Chemistry Webbook, NIST Standard Reference Database Number 69*; Linstrom, P. J., Mallard, W. G., Eds.; National Institute of Standards and Technology: Gaithersburg, MD, 2003; http://webbook.nist.gov.
(32) (a) Scheidt, W. R.; Ellison, M. K. *Acc. Chem. Res.* **1999**, *32*, 350. (b) Gorbunov, N. V.; Osipov, A. N.; Day, B. W.; Zayas-Rivera, B.; Kagan, V. E.; Elsayed, N. M. *Biochemistry* **1995**, *34*, 6689.

pathway of the NO adduct, $[(TPFPP)Fe^{III}NO]^+$, from the reaction of **1** with NO_2.[25b,33]

To shed further light on the mechanism of this process, we assayed the interaction of the putative intermediate **3** with NO_2. Surprisingly, the only observed product ion was **1**, indicative of an oxygen atom transfer from **3** to give NO and O_2 as likely products (eq 4), a process found to be moderately efficient ($\phi = 2.0\%$).

$$\mathbf{3} + NO_2 \rightarrow \mathbf{1} + [NO + O_2] \qquad (4)$$

With inspection of the data reported in Table 1, it is evident that whereas alkanes and benzene are not activated by **3**, alkenes (S = *cis*- and *trans*-2-butene, cyclohexene) do react with moderate efficiencies and similar branching ratios for the formation of product ions. Oxidation of olefins represents a fundamental issue in biological and synthetic transformations. Several gas-phase investigations have focused on the oxygen atom transfer to ethylene by transition metal oxides MO^+, showing that the more stable product acetaldehyde is formed rather than oxirane.[15a] However, when a ligated metal oxide $[(C_6H_6)FeO]^+$ was assayed, a quite different reactivity toward olefins was observed, leading to the neutral epoxide rather than to carbonyl compounds.[30] In analogy with this finding, it is likely that epoxide products are formed also in the present experiments.

The competitive epoxidation of *cis*- vs *trans*-olefins has been used in solution as a mechanistic probe to investigate the influence of anionic ligands, X^-, bound to iron porphyrin complexes on the oxidizing power and/or lifetime of the reactive intermediates. Interestingly, the similar yields of *cis*- vs *trans*-butene oxide products found in our experiments (cis/trans = 1.2, Table 1), where **3** reacts with *cis*- and *trans*-2-butene in the absence of any X^-, compare well with the low ratios of *cis*- to *trans*-stilbene oxide products measured in solution with nonligating or weakly ligating (i.e. $CF_3SO_3^-$, ClO_4^-) counterions (cis/trans = 0.9).

S-oxidation of thioethers to sulfoxides is promoted by high-valent oxoiron intermediates both in synthetic and enzymatic reactions.[8g,26b] Recently, it has been reported that reduction of easily accessible compound I by sulfides proceeds via a direct oxygen transfer mechanism rather than by sequential electron transfer.[34] In the present study, besides the formation of an addition product $[(TPFPP)Fe(Me_2S)O]^+$ (70%), sulfur−O bond coupling in dimethyl sulfide yields **1** (30%). Despite a $\Delta_f H°$ difference favoring Me_2SO with respect to Me_2S by about 115 kJ mol^{-1}, the oxidation of Me_2S is nevertheless not activated by free FeO^+ probably due to the competition of more favorable channels.[15e] Noteworthily, the presence of the porphyrin ligand accounts for a quite different reactivity behavior of **1** as compared to free FeO^+.

The main reaction pathway of **3** with trimethyl phosphite yields **1** (90%), suggesting the formation of a phosphorus−O bond to afford trimethyl phosphate, by analogy with the **3**/Me_2S system. The difference between $\Delta_f H(MeO)_3PO$ and $\Delta_f H(MeO)_3P$) favors the phosphate product by about 409 kJ mol^{-1}, and the high relative yield efficiency ($\phi = 49\%$) is in line with the high oxophilicity of trivalent phosphorus.

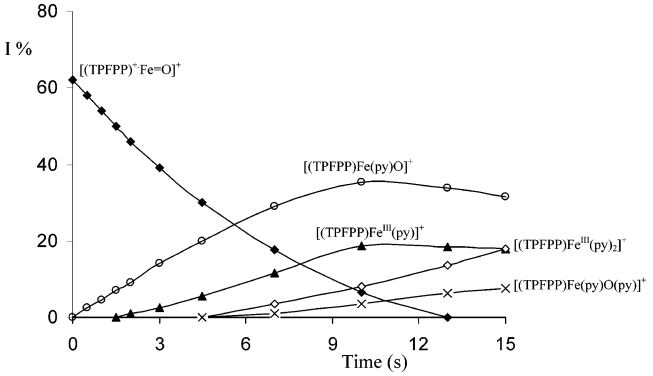

Figure 3. Time dependence of ion abundances for the reaction of $[(TPFPP)^{\bullet+}Fe^{IV}{=}O]^+$ at $m/z = 1044$ (◆) with C_5H_5N (py) at 7.1×10^{-8} mbar. Products ions are $[(TPFPP)Fe(py)O]^+$ at $m/z = 1123$ (○), $[(TPFPP)Fe^{III}(py)]^+$ at $m/z = 1107$ (▲), $[(TPFPP)Fe^{III}(py)_2]^+$ at $m/z = 1186$ (◇), and $[(TPFPP)Fe(py)O(py)]^+$ at $m/z = 1202$ (×).

As already stated, the reaction of **3** with sampled amines (S = dimethylamine, pyridine) proceeds uniquely by an addition route with similar efficiencies (eq 2b, Table 1). The time dependence of ion abundances is exemplified by the pyridine reaction (Figure 3). However, the kinetic plot reveals that the primary product $[(TPFPP)Fe(C_5H_5N)O]^+$ reacts further with the neutral showing two distinct reaction routes: (1) association of pyridine to form $[(TPFPP)Fe(C_5H_5N)_2O]^+$; (2) displacement of a formal pyridine oxide unit (C_5H_5NO) by pyridine to yield $[(TPFPP)Fe(C_5H_5N)]^+$, which then undergoes addition of another pyridine molecule eventually giving the bis-ligated complex $[(TPFPP)Fe(C_5H_5N)_2]^+$. The difference between the $\Delta_f H(C_5H_5NO)$ and $\Delta_f H(C_5H_5N)$ favors pyridine oxide by 52.3 kJ mol^{-1}. All available evidence convincingly points against the individual interaction of an amine ligand at the iron center within the primary adduct $[(TPFPP)Fe(C_5H_5N)O]^+$, i.e., against the presence of two distinct oxo and pyridine axial ligands. Rather, the formation of an oxidized product can be inferred both from the pyridine for pyridine *N*-oxide ligand exchange and from the addition of pyridine at the still free sixth coordination site within $[(TPFPP)Fe(C_5H_5NO)]^+$. Ultimately, the latter adduct resembles the ones formed in solution by the reaction of manganese porphyrin or salen complexes with amine *N*-oxides.[35]

In the following sections a deeper insight into the features of product ions from reaction 2 is attempted.

Ligand Association Reactions to $[(TPFPP)Fe^{III}]^+$ (1). The reaction of **1** with selected ligands (L) yields the association product ions, $[(TPFPP)Fe^{III}L]^+$ (eq 5). In the

$$\mathbf{1} + L \underset{k_{diss}}{\overset{k_{coll}}{\rightleftharpoons}} [(TPFPP)Fe^{III}L]^+_{exc} \xrightarrow{k_r} [(TPFPP)Fe^{III}L]^+ \qquad (5)$$
$$k_{term}[L]$$

highly dilute environment that is experienced by the ions in the cell of the FT-ICR instrument, an excited complex

(33) Chen, O.; Groh, S.; Liechty, A.; Ridge, D. P. *J. Am. Chem. Soc.* **1999**, *121*, 11910.
(34) Goto, Y.; Matsui, T.; Ozaki, S.; Watanabe, Y.; Fukuzumi, S. *J. Am. Chem. Soc.* **1999**, *121*, 9497.

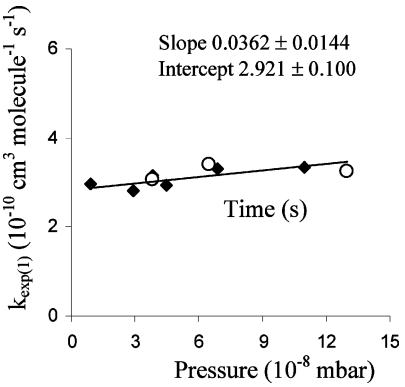

Figure 4. Rate constants ($k_{exp(1)}$) for the addition reaction between $[(TPFPP)Fe^{III}]^+$ and nitric oxide as a function of NO pressure, varied over the range $9.0 \times 10^{-9}-1.1 \times 10^{-7}$ mbar, without (◆) and with (○) added buffer gas (Ar at $1.5 \times 10^{-8}-1.2 \times 10^{-7}$ mbar).

$[(TPFPP)Fe^{III}L]^+_{exc}$ is formed at the collision rate, k_{coll}, owning an excess internal energy corresponding to the adduct binding energy. This hot complex will not survive to a rapid back-dissociation, k_{diss}, unless stabilized by radiative emission of IR photons, k_r, and/or by third-body collisions, k_{term} (eq 5). At low pressure, radiative stabilization may become the prevailing mechanism. The relative contribution of the two thermalization phenomena may be derived by a pressure dependence study of the apparent rate constant for the association process. Radiative association kinetics can then be extrapolated to zero pressure and used, along with suitable modeling, to deduce accurate estimates of binding energies, as reported for several reactions leading to gaseous metal−ligand complexes and proton-bound dimers.[36] The binding energy of NO to heme cations has been recently estimated to be ca. 24.8 ± 0.7 kcal mol^{-1} by modeling of the radiative association rates.[33] Figure 4 shows the kinetic results for the addition reaction of NO to **1** as a function of ligand (L = NO) pressure, varied over the range $9.0 \times 10^{-9}-1.1 \times 10^{-7}$ mbar, and of an additional pressure of buffer gas (Ar at $1.5 \times 10^{-8}-1.2 \times 10^{-7}$ mbar). Within the pressure range explored, radiative emission is the primary stabilization mechanism operative in the association reactions tested in this study. The selected ligands, chosen to provide models of substrates or amino acid residues of heme enzymes, are listed in Table 2 according to their increasing efficiency, $\phi_{(1)}$ for the radiative association kinetics, which spans from 73% for trimethyl phosphite to 3.4% for NO. Noteworthily, the radiative association rate with NO ($k_{exp} = (0.35 \pm 0.12) \times 10^{-10}$ cm^3 molecule^{-1} s^{-1}) compares well with the value reported for a gaseous heme cation ($k_{exp} = (0.15 \pm 0.05) \times 10^{-10}$ cm^3 molecule^{-1} s^{-1}) and for a related model complex, a singly protonated iron tetrapyridylporphyrin ($k_{exp} = (0.48 \pm 0.15) \times 10^{-10}$ cm^3 molecule^{-1} s^{-1}).[33]

When the sampled neutral is a strong ligand, the sequential addition of a second neutral molecule (eq 6) to form six-coordinated complexes is also observed (L = Me_2NH, C_5H_5N, $(MeO)_3P$) and measured ($k_{exp(2)}$ and $\phi_{(2)}$ are given in Table 2).

$$[(TPFPP)Fe^{III}L]^+ + L \rightarrow [(TPFPP)Fe^{III}L_2]^+ \qquad (6)$$

Interestingly, the observation that this route (eq 6) proceeds at lower efficiencies as compared to the first addition process (eq 5) proves that the electrophilic character of the reactant ion is sensitive to the electron-donating ability of the first ligand associated with the iron porphyrin complex.

Inspection of the data reported in Table 3 suggests that the reactivity of **1** toward L *roughly* parallels the proton affinity (PA) of lone pair donor ligand; that is, both the efficiency and the extent of ligation increase with ligands endowed with higher PA values.[31] This positive trend may reflect the involvement of similar features in stabilizing the adducts of L with both electrophiles, either the proton or the iron(III) porphyrin complex. In contrast with the behavior of some inert ligands (L = O_2, CO, cyclohexane, and olefins), whose reactivity was too low to be observed ($k_{exp} \leq 10^{-12}$ cm^3 molecules^{-1} s^{-1}), the interaction of nitrogen oxide is remarkably effective despite its low PA, in accord with its unique role in the heme-proteins' physiology. Some other less pronounced deviations may be accounted for by the electrostatic contribution to the coordinative bonding. For example, dimethylamine appears less effective than compounds of similar basicity but higher dipole moment such as pyridine and trimethyl phosphite (μ(dimethylamine) = 1.0 D; μ(pyridine) = 2.2 D; μ(trimethyl phosphite) = 3 D). When these effects cannot come into play, comprehensive

Table 2. Kinetics of Radiative Association Reactions of $[(TPFPP)Fe^{III}]^+$ (**1**) with Selected Ligands L

L (PA)[a]	$k_{exp(1)}$[b−d]	$\phi_{(1)}$[e]	$k_{exp(2)}$[b,f]	$\phi_{(2)}$[e]
NO (531.8)	0.35	5.0		
NO_2 (591)	0.25[g]	3.4		
Me_2S (830.9)	0.69	5.4		
Me_2NH (929.5)	2.5	22	0.12	1.1
C_5H_5N (930)	4.5	33	0.30	2.2
$P(OMe)_3$ (929.7)	8.2	73	4.1	37

[a] Proton affinities (PA) in kJ mol^{-1} are given in parentheses. [b] See footnote *b* in Table 1. [c] The following reactants failed to react with $[(TPFPP)Fe^{III}]^+$: O_2; CO; cyclohexane; cyclohexene; (*Z*)-2-butene; (*E*)-2-butene; N_2O. [d] Reaction step: $[(TPFPP)Fe^{III}]^+ + L \rightarrow [(TPFPP)Fe^{III}L]^+$. [e] See footnote *d* of Table 1. [f] Reaction step: $[(TPFPP)Fe^{III}L]^+ + L \rightarrow [(TPFPP)Fe^{III}L_2]^+$. [g] The NO_2 reaction leads to $[(TPFPP)Fe^{III}(NO)]^+$ as the only observed product ion.

Table 3. Gas-Phase Ligand Exchange Reactions of $[(TPFPP)Fe(S)O]^+$ Adduct Ions Generated in Solution and in the Gas Phase with Selected Neutrals (L)

substrate (S)	phase	L	k_{exp}[a]	ϕ[b]	product ions $[(TPFPP)Fe^{III}L]^+$/ $[(TPFPP)Fe(S)O(L)]^+$
c-C_6H_{10}	gas	Me_2NH	2.5	29	80/20[c]
Me_2NH	gas	C_6H_5N	0.91	7.0	100/0
Me_2S	gas	C_6H_5N	0.59	4.4	80/20
Me_2S	gas	Me_2NH	0.31	2.6	80/20
Me_2S	solutn	Me_2NH	0.15	1.6	70/30
PhSMe	solutn	Me_2NH	nd[d]	nd[d]	0/100

[a] See footnote *b* in Table 1. [b] See footnote *d* in Table 1. [c] In this case a dissociation route was observed, affording $[(TPFPP)Fe^{III}]^+$. [d] nd stands for not detected; PA(PhS(O)Me) = 926.2−932 kJ mol^{-1}, estimated by the additivity group rule.

(35) (a) Srinivasan, K.; Michaud, P.; Kochi, J. K. *J. Am. Chem. Soc.* **1986**, *108*, 2309. (b) Powell, M. F.; Pai, E. F.; Bruice, T. C. *J. Am. Chem. Soc.* **1984**, *106*, 3277.

(36) (a) Ho, Y.-P.; Yang, Y.-C.; Klippenstein, S. J.; Dunbar, R. C. *J. Phys. Chem. A* **1997**, *101*, 3338. (b) Ryzhov, V.; Dunbar, R. C. *J. Am. Soc. Mass Spectrom.* **1999**, *10*, 862. (c) Fridgen, T. D.; McMahon, T. B. *J. Am. Chem. Soc.* **2002**, *106*, 1576.

correlations can be found between the binding energy of extended series of compounds toward either NO^+ or NO_2^+ and their PA values.[37]

Ligand Transfer Reactions by [(TPFPP)Fe(S)O]$^+$ (6). To clarify if also other substrates, in addition to pyridine, undergo O-bond formation upon activation within the addition complex (eq 2b), the structural characterization of some exemplary adducts **6** was attempted by assaying their gas-phase reactivity toward selected L (Table 3). Ions **6** were prepared in good yields either by ion−molecule reactions in the gas phase (eq 2b) or by electrospray of in situ mixtures of **1**-Cl/H_2O_2 and substrate S in methanol. Concerning the reaction carried out in solution, although the intermediacy of related complexes has been frequently invoked (for example in PhIO-mediated oxidations), the formation of an iodosylbenzene−iron porphyrin adduct has only recently been demonstrated in the reaction of $[(Porp)^{\bullet+}Fe^{IV}{=}O]^+$ with various substituted iodobenzenes and found to depend on the electronic features of both reactants.[8b] Herein, the electron-poor porphyrin ligand is expected to reduce the reactivity of the oxoiron center, and indeed, several adducts $[(TPFPP)Fe(S)O]_{sol}^+$ (S = Me_2S, PhSMe, PPh_3) have been formed in solution. A noticeable exception is presented by S = PhI. This substrate did not yield any $[(TPFPP)Fe(S)O]_{sol}^+$ but rather caused reduction of **3** to afford **1**.

In the case that genuine adducts with distinct oxo (O) and substrate (S) ligands were formed, a displacement process of an intact S molecule is expected to occur by a neutral L with a larger affinity for the complexed metal ion as compared to S. Interestingly, no product species corresponding to a neat replacement of S by L was observed (eq 6a); rather, in all investigated systems an intact SO unit was replaced by L (eq 6b) until complete reactant consumption. This outcome demands that an O-coupling has occurred from the high-valent iron oxo intermediate **3** to an oxophilic site of S within the $[(TPFPP)Fe(S)O]^+$ complex. It may then be inferred that routes (2a) and (2b) both conform to the whole oxidative ability of **3** in the gas phase. In a minor addition pathway $[(TPFPP)Fe(S)O(L)]^+$ ions are formed (eq 6c), where the details of the bonding of both S and L are not yet assayed.

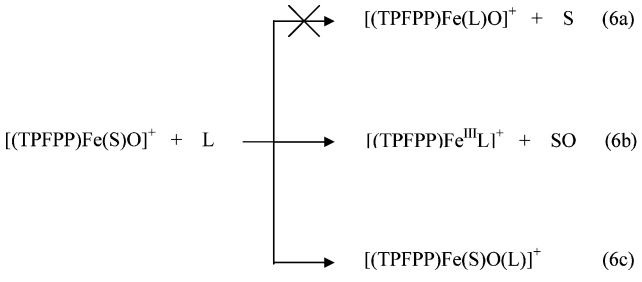

The main channel (eq 6b) can be envisioned as the transfer of ion **1** from SO to a neutral molecule L, whose affinity for **1** exceeds that of SO. From the correlation between the association efficiency and ligand PA noted above, dimethylamine and pyridine have been chosen as appropriate neutrals to assay reaction 6 in the gas phase. Indeed, as the difference between $PA_{(L)}$ and $PA_{(SO)}$, ($\Delta PA(L/SO)$) increases, the ligand exchange reaction becomes more efficient. For example, when $\Delta PA(Me_2NH/PhS(O)Me)$ is $-2.5 \div 3.4$ kJ mol^{-1}, ϕ is unmeasurably small; when $\Delta PA(Me_2NH/Me_2SO)$ is 45.1 kJ mol^{-1}, ϕ is 2.2%. Finally, when $\Delta PA(Me_2NH/C_6H_{10}O)$ is 81.4 kJ mol^{-1}, ϕ is 23.2%.[31]

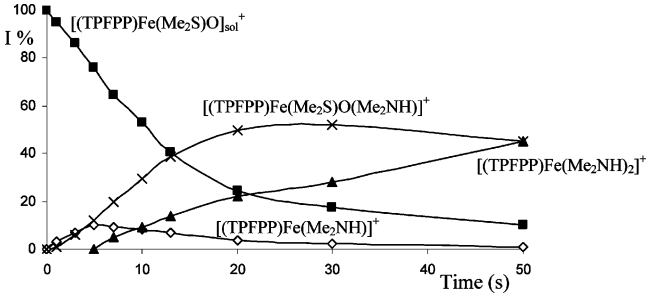

Figure 5. Time dependence of relative ion intensities when $[(TPFPP)Fe(Me_2S)O)]_{sol}^+$ ions at $m/z = 1106$ (■) are allowed to react with Me_2NH (7.5×10^{-8} mbar) yielding $[(TPFPP)Fe(Me_2S)O(Me_2NH)]^+$ at $m/z = 1151$ (×), $[(TPFPP)Fe(Me_2NH)]^+$ at $m/z = 1073$ (◇), and $[(TPFPP)Fe(Me_2NH)_2]^+$ at $m/z = 1118$ (▲).

The results shown in Table 3 point out that association complexes $[(TPFPP)Fe(S)O]^+$ generated either in solution or in the gas phase show similar behavior, as evidenced by the comparable values of branching ratios for the formation of product ions. Obvious differences are observed when S is cyclohexene, whose lack of reactivity toward addition confirms the limited binding energy to **1**, as already noted, and when S is thioanisole, whose oxidized product, methyl phenyl sulfoxide, does not undergo substitution by dimethylamine, in line with thermochemical considerations that predict the process to be unfavorable. Attempts to investigate the reactivity behavior of $[(TPFPP)Fe(S)O]_{sol}^+$ with S = PPh_3 toward pyridine showed a ligand exchange product (route 6b), but an accurate measurement of the rate constant was hampered owing to the instability of the species in the parent solution. On the other end, the scant volatility of this highly oxophilic compound did not allow production of the corresponding $[(TPFPP)Fe(S)O]_{gas}^+$.

Figure 5 shows an exemplary ion intensity profile for the reaction of dimethylamine with $[(TPFPP)Fe(Me_2S)O]_{sol}^+$. It is evident that the primary products, $[(TPFPP)Fe^{III}(Me_2NH)]^+$ and $[(TPFPP)Fe^{III}(Me_2S)O(Me_2NH)]^+$, formed by the exchange (eq 6b) and addition (eq 6c) routes, respectively, react further with the neutral. Whereas addition at the sixth coordinative position of $[(TPFPP)Fe^{III}(Me_2NH)]^+$ yields the bis-adduct $[(TPFPP)Fe^{III}(Me_2NH)_2]^+$, the association complex $[(TPFPP)Fe^{III}(Me_2S)O(Me_2NH)]^+$ may undergo ligand substitution with the neutral, eventually giving $[(TPFPP)Fe^{III}(Me_2NH)_2]^+$ and Me_2SO. The latter pathway was independently demonstrated upon selection of $[(TPFPP)Fe^{III}(Me_2S)O(Me_2NH)]^+$ in the presence of dimethylamine at 7.5×10^{-8} mbar. Notably, when $[(TPFPP)Fe^{III}(Me_2S)O]_{sol}^+$ or $[(TPFPP)Fe^{III}(Me_2S)O]_{gas}^+$ were allowed to react with the same neutral L = Me_2NH, comparable branching ratios and efficiencies were measured. Kinetic analysis of the ion intensity plots sets the possible presence of unreactive

(37) Cacace, F.; de Petris, G.; Pepi, F. *Proc. Natl. Acad. Sci. U.S.A.* **1997**, *94*, 3507.

isomeric forms at an upper limit of 10%. This evidence suggests that the mechanism of oxygen atom transfer to the substrate might be governed by similar factors both in solution and in the gas phase, besides confirming electrospray ionization as a soft and efficient tool for transferring metal ion complexes and reaction intermediates to the gas phase without apparently altering their intrinsic features.

Conclusion

In summary, the following picture emerges from our ESI-FT-ICR experiments. Electrosprayed high-valent iron(IV) oxo porphyrin cation radical **3** is able to promote O-atom release to appropriate substrates S in the gas phase, thus affording $[(TPFPP)Fe^{III}]^+$ (**1**) and SO. On the basis of the way **3** is formed, this reaction ultimately represents an approach to stoichiometric oxidations by the abstraction of an oxygen atom from hydrogen peroxide. Because the heat of formation of **3** is not available, the actual thermochemistry of each process could not be evaluated. Nevertheless, the difference between $\Delta_f H°$(SO) and $\Delta_f H°$(S), together with the first ionization potential (IP) of S reported in Table 1, may be related to the propensity of S to undergo cytochrome P450 mediated oxidations. Indeed, the reaction efficiencies show some correlation with the above parameters and increasing yields are obtained when oxophilic centers (C > S > P) are present. The reactivity of pyridine, however, matches or even overwhelms that of nitric oxide, olefins, and dimethyl sulfide despite the less favorable thermodynamics. This finding may be explained by ion−dipole interactions within the complex that may favor ligands with high values of dipole moment ($\mu_D(C_5H_5N) = 2.25$ D). In line with the prominent biological role of NO/iron porphyrin complexes, NO displays a unique behavior, being highly reactive despite its low PA value and dipole moment. The reaction efficiencies as well the branching ratio of product ions seem thus to derive from a balance of energetic constrictions and physicochemical properties of the investigated substrates.

Several ligands react with **1** by a radiative association process with reaction efficiencies showing a general positive trend with their PA values.

ESI-FT-ICR has proven to be a convenient approach to isolate and characterize ionic intermediates active in biomimetic iron(III) porphyrin catalyzed oxygenations by hydrogen peroxide in solution. The intrinsic reactivity of an oxoiron(IV) porphyrin cation radical complex, **3**, a model of the putative active species in the catalytic cycle of heme enzymes, has been measured in the gas phase beyond the complication of solvation and ion-pairing. To take advantage of the ion manipulation versatility of FT-ICR, elementary steps in the mechanism of the oxidation reaction were tested allowing a comparison between gas phase and solution chemistry. These results may be valuable for the construction of unified models of transition metal catalysis.

Acknowledgment. This project was supported by the Italian Ministero dell'Istruzione, dell'Università e della Ricerca.

IC048595C